Published in final edited form as:
Curr Biol. 2010 January 26; 20(2): 182–187. doi:10.1016/j.cub.2009.11.072.

Identification of signaling pathways regulating primary cilium length and flow-mediated adaptation

Tatiana Y. Besschetnova[1,4], **Elona Kolpakova-Hart**[2,3], **Yinghua Guan**[1,4], **Jing Zhou**[4], **Bjorn R. Olsen**[2,3], and **Jagesh V. Shah**[1,4,5,*]

[1] Department of Systems Biology, Harvard Medical School, Boston, MA, USA

[2] Department of Cell Biology, Harvard Medical School, Boston, MA, USA

[3] Department of Oral and Developmental Biology, Harvard School of Dental Medicine, Boston, MA, USA

[4] Renal Division, Department of Medicine, Brigham and Women's Hospital, Boston, MA, USA

[5] Harvard-MIT Division of Health Sciences and Technology, Boston, MA, USA

Summary

The primary cilium acts as a transducer of extracellular stimuli into intracellular signaling [1,2]. Its regulation, particularly with respect to length, has been defined primarily by genetic experiments and human disease states in which molecular components that are necessary for its proper construction have been mutated or deleted [1]. However, dynamic modulation of cilium length, a phenomenon observed in ciliated protists [3,4], has not been well-characterized in vertebrates. Here we demonstrate that decreased intracellular calcium (Ca^{2+}) or increased cyclic AMP (cAMP), and subsequent PKA activation, increases primary cilium length in mammalian epithelial and mesenchymal cells. Anterograde intraflagellar transport is sped up in lengthened cilia, potentially increasing delivery flux of cilium components. The cilium length response creates a negative feedback loop whereby fluid shear-mediated deflection of the primary cilium, which decreases intracellular cAMP, leads to cilium shortening and thus decreases mechanotransductive signaling. This adaptive response is blocked when the autosomal dominant polycystic kidney disease (ADPKD) gene products, polycystin-1 or -2, are reduced. Dynamic regulation of cilium length is thus intertwined with cilium-mediated signaling and provides a natural braking mechanism in response to external stimuli that may be compromised in PKD.

Keywords

Primary cilium; cyclic AMP; Length regulation; Polycystins; Calcium

[*]Correspondence and request for materials should be addressed to J.V.S. (Jagesh_Shah@hms.harvard.edu), Address: Harvard Institutes of Medicine, 4 Blackfan Circle, Room 564, Boston, MA, 02115, USA, Phone: +1 (617) 525-5912.

Competing Interests
The authors declare no competing interests.

Authors Contributions
T.Y.B. and J.V.S. designed the experiments. T.Y.B., Y.G. and J.V.S. performed the experiments. T.Y.B., E.K-H., B.R.O and J.V.S. generated reagents. J.Z. provided reagents. T.Y.B., B.R.O., and J.V.S, wrote the manuscript.

Results and Discussion

To test the potential role of known signaling pathways in governing cilium length we carried out a small-scale screen of bioactive compounds with known targets to test their ability to acutely increase cilium length (i.e. within three hours). Our screen utilized the immortalized kidney collecting duct line (IMCD) [5], embryonically derived kidney epithelia (MEK) [6] and primary bone mesenchymal cells (BME) [7]. These cells were chosen for their robust formation of primary cilia upon reaching confluence in cell culture, as observed by indirect immunofluorescence microscopy (Figures 1A,S1A, S1C). Two major classes of compounds emerged as potent stimulators of cilium length in all three cell types: molecules directed at blocking Ca^{2+} entry into cells or release of intracellular Ca^{2+} stores (e.g. Gd^{3+}) and those increasing intracellular cyclic AMP (e.g. forskolin [8]). These compounds increased cilium length almost two-fold in three hours (Figures 1A and 1B). In IMCD cells cilia length increased from 6.0 ± 0.4 to 10.7 ± 1.75 and 11.7 ± 1.1 μm (mean ± s.d.) after Gd^{3+} and forskolin treatment, respectively. Similar results were seen in both MEK and BME cells (Figure 1C, S1B and S1D).

Using a number of compounds that modulate levels of intracellular second messengers, we were able to further explore the effect of Ca2+ and cAMP on cilium length (Figure 2A). The ryanodine receptor inhibitor dantrolene, which acts to prevent Ca^{2+} release, increased cilium length. In contrast, releasing intracellular calcium stores (e.g. Thapsigargin) or activation of polycystin-2, a Ca^{2+} permeable, non-selective cation channel, via triptolide [9] modestly decreased cilium length. Use of a cAMP analogue, 8-Br-cAMP, which directly activates protein kinase A/cAMP-dependent kinase (PKA) also increased cilium length. Conversely, a competitive inhibitor of PKA activation Rp-cAMPS or direct inhibition of PKA by H-89 or KT5720 resulted in shortening of the cilium (Figure 2A). Thus increasing intracellular cAMP and subsequent downstream activation of PKA acted to increase cilium length and inhibition of PKA activity reduced cilium length and the converse being observed for intracellular Ca^{2+}.

Inhibition of phosphodiesterase activity had no significant effect on cilium length (Figure S2A) indicating that a constitutive cAMP degradation activity is not acting in these cells over the time course of our experiment. Compounds targeting cGMP-mediated pathways did not modulate mammalian primary cilium length (Figure S2B) in contrast to its effect on nematode sensory neurons [10].

The increase in cilium length did not require protein synthesis since each drug was effective in the presence of cycloheximide, a protein synthesis inhibitor (Figure S2C). In addition, the length increase was reversed by either removal of the drug after treatment (data not shown) or by chelation of Gd^{3+} by addition of stoichiometric concentrations of EGTA (30μM, much less than required for Ca^{2+} chelation) after the initial length increase (Figure S2D).

To ascertain potential crosstalk between the signaling pathways we measured the levels of second messengers directly after administration of the two most potent compounds, forskolin and Gd^{3+}. Measurements of steady-state intracellular cAMP levels were increased 2-fold by Gd^{3+} and 6-fold by forskolin in comparison to untreated cells (Figure 2B). Steady-state intracellular Ca^{2+} levels were reduced 43% and 37% when cells were treated with Gd^{3+} and forskolin, respectively (Figure 2C). Together these data reveal the crosstalk between Ca^{2+} and cAMP and suggest that their coordinate regulation modulates cilium length and that they may converge on a common final effector.

Titration of the forskolin response with a specific PKA inhibitor prevented cilium-lengthening indicating that PKA is the downstream element in the cAMP-mediated cilium length regulation (Figures 2D and S2E). PKA inhibition also prevented Gd^{3+}-induced cilium

length increase. Conversely, Thapsigargin suppressed the effect of forskolin cilium lengthening but had no effect on 8-Br-cAMP-induced cilium lengthening (10.96 ± 1.09 and 9.32 ± 1.59 μm under 8-Br-cAMP and 8-Br-cAMP plus Thapsigargin incubation, respectively, Figures 2D and S2F), indicating a potential role for Ca^{2+} modulation of adenylyl cyclases. To investigate the role of adenylyl cyclases (AC) in this pathway, we used short-interfering RNAs to knockdown the expression of AC5 and AC6, two isoforms found in our cell lines and inhibited by Ca^{2+} [11] (Figures S2G and S2H). The knockdown of AC5 and AC6 both blocked cilium lengthening via Gd^{3+} (i.e. acting via Ca^{2+}) but not via 8-Br-cAMP (i.e. direct PKA activation) (Figures 2E and S2I). Together these data support a pathway by which cilium length is increased downstream of PKA activation that is increased by direct activation (8-Br-cAMP), through release of AC5/6 inhibition via reduced intracellular Ca^{2+} or AC activation by forskolin. This pathway is active in cells of epithelial and mesenchymal origin underscoring a generalized control of primary cilium length in many tissues.

To investigate mechanisms by which PKA may regulate cilium length, we observed the delivery of constituent proteins to the cilium by imaging the intraflagellar transport (IFT) machinery [12]. IFT particles are transported along axonemal microtubules towards the cilium tip (anterograde) and removed by transport towards the cell body (retrograde). Cilium length regulation requires coordinate regulation of particle trafficking, size, frequency and speed to modulate the particle flux [3]. We visualized IFT particle trafficking by labelling an IFT component, IFT88, with EYFP (Figures 3A and 3B and supplemental movies) [13]. Upon addition of compounds to increase cilium length, anterograde IFT88 particle velocities increased by ~70%. In contrast, there were no significant effects on retrograde velocities (Figures 3C, 3D and 3E). Moreover, the lengthened cilia displayed greater fluorescence at the tip indicating accumulation of IFT88 consistent with an increased anterograde and unchanged retrograde velocities (Figure 3B). This increase in anterograde velocity of transport, without a significant change in retrograde velocity, could result in an increase in material flux into the cilium thereby leading to increased length. However, the material flux is derived from a number of parameters such as particle number, size and occupancy that we have not measured here requiring a more detailed analysis to understand the contribution of increased anterograde velocity to the length increase.

The dynamic modulation of particle velocity has not previously been reported in mammalian cells (for Chlamydomonas see [14]) and represents a novel form of control for cargo transport. One possible mechanism at work can be inferred from studies of the nematode cilium where two motors, Kinesin-II and OSM3, both contribute to IFT but move at different velocities [15]. Ablation of Kinesin-II, the slower motor (and in a mutant bbs background), results in all IFT particles moving at the faster OSM3 velocity and the ablation of OSM3 (again in a bbs mutant background) results in all IFT particles moving at the slower Kinesin-II velocity. A mechanism to dynamically titrate motor stoichiometries on IFT particles could be used to regulate particle velocity. In addition to motor-IFT composition, there may also exist some enzymatic modulation of the motor itself or modification of the microtubule track [16] that may impact IFT transport. Recent work from Engel and colleagues demonstrates that motor velocity changes as a function of length in regenerating Chlamydomonas flagella after pH shock[14]. Their work suggests that flagellar length may itself be upstream of motor velocity control rather than downstream, as we have proposed. Further study will be required to identify the underlying mechanisms of increased anterograde IFT particle velocity.

The dynamic control of cilium length which we have observed could provide a unique regulatory mechanism for the control of sensitivity to extracellular cues. Given the similarity in co-regulation of intracellular Ca^{2+} and cyclic AMP between cilium length control and

flow mechanotransductive signaling [17,18], we tested the effect of flow on cilium length. Primary cilia in a number of tissues, most notably the kidney tubule and hepatobiliary tree, transduce low shear stress fluid flow via cilium deflection and Ca^{2+} influx [19]. After exposing kidney-derived IMCD and MEK epithelial cells to three hours of shear stress (0.75 dyne/cm^2) we found that untreated cells and those treated with forskolin underwent significant decreases (20–35%, $P<0.05$) in cilium length (Figure 4A). Moreover, intracellular cyclic AMP levels were also significantly decreased (1.5–3 fold) under flow, even in the presence of forskolin as previously described by Masyuk and colleagues [18], and are consistent with the observed cilium length reduction (Figure 4C). Similar results were also observed in wild-type MEK cells (Figures 4B and 4D). The effect of cilium length reduction would reduce the length of the lever arm and decrease the sensitivity to fluid shear stress creating a previously unappreciated negative feedback loop to adapt intracellular signaling to external cues.

Interestingly, Gd^{3+} treatment blocked the cilium length decrease under flow and the reduction in cyclic AMP levels (Figures 4C and 4D). The action of Gd^{3+} is rather promiscuous; however, it has been shown to block the activity of polycystin-2 (PC2), a TRP channel involved in Ca^{2+} entry under flow-mediated shear stress [20]. We investigated the role of PC2 and its binding partner polycystin-1 (PC1) as regulators of cilium length since both are known to regulate flow mechanotransduction and found mutated in autosomal dominant forms of polycystic kidney disease (ADPKD) [21]. IMCD cells stably knocked down for PC2 (to ~20% of wild-type levels, Figure S4A) were subjected to flow but did not exhibit the cilium length decrease as seen in their parental counterparts under untreated conditions or forskolin addition (Figure 4E). As expected from the lack of cilium length modulation, these cells were unable to decrease cAMP levels under flow (Figure 4G). Furthermore, these cells exhibited a hyperactive cAMP response to forskolin (~2.5 fold over wild-type cells) that was maintained in the presence of flow. We tested the role of PC1 via MEK cell lines generated from mice with a mutation (del34) in the gene encoding for PC1 [6] (Figure S4B). Like the PC2 knockdown cells, these cells did not exhibit length decrease or a decrease in intracellular cyclic AMP under flow, indicating a role for polycystins in cilium length adaptation (Figures 4F and 4H). Notably, cells mutated for PC1 or knocked down for PC2 all responded to forskolin in a similar fashion to wild-type cells, with respect to cilium length, under static conditions but did not undergo cilium length increase upon administration of Gd^{3+}. The response of wild-type cells to Gd^{3+} might be expected to act like knockdown of PC1/PC2, given the reduced Ca^{2+} level (Figures S4E and S4F). However there was no difference in untreated cilium lengths for cells wild-type or reduced PC1/PC2 function (Figures 4A and 4E). This suggests that cells can adapt cilium length via an as yet unidentified mechanism under chronic conditions (e.g. mutation or long-term knock-down) but that acute perturbations of Ca^{2+} homeostasis (e.g. via Gd3+ administration) modulate cilium length via the activity of PC1/PC2.

Dynamic cilium length regulation has been observed in a number of unicellular ciliates, for example in *Chlamydomonas* after deflagellation [4,22]. However, the dramatic and reversible cilium length increase seen here has not been previously studied in mammalian cells and even remains poorly understood in unicellular ciliated organisms. The data presented here demonstrate that modulation of intracellular Ca^{2+} and cyclic AMP and its downstream activation of PKA controls cilium length in part by regulating IFT particle transport velocity and possibly material anterograde flux. This second messenger-mediated control regulates cilium length downstream of cellular signals such as flow-induced mechanotransduction, reducing sensitivity to fluid shear by decreasing cilium length. The ADPKD proteins PC1 and PC2 regulate this adaptation and in their absence cells are unable to down-regulate cAMP and thus cilium length remains unchanged.

This novel form of mechanical adaptation acts to modulate the response to fluid shear and potentially other extracellular cues. Polycystins act as a brake on signaling. In their absence, signaling would continue unabated. The regulation of signaling by flow-induced mechanotransduction has been widely hypothesized as a mechanism that may be defective in PKD [23]. Moreover, careful studies from the Verghese and colleagues indicate that renal tubular cilia length is modulated during various forms of renal injury and repair ([24,25] and our own unpublished results), implicating dynamic length regulation as part of a regenerative program. Given that these injury models themselves can act to potentiate cystogenesis in mouse models of PKD [26–28], it is appealing to speculate that dynamic cilium length regulation may be a part of an anti-cystogenic repair program, that when absent contributes to cystic pathology.

Experimental Methods

Live Cell Imaging of Intraflagellar Transport

Velocity measurements of IFT particles were performed as described previously [13]. Briefly, m368-4 (clonal line of IMCD cells stably expressing IFT88-EYFP) cells were cultured on 18-mm poly-L-lysine-coated coverslips in DMEM/10% FBS. A confluent monolayer of cells was subjected to IFT transport analysis by inversion onto a large coverslip and a drop of CO_2-independent media (Invitrogen, Carlsbad, CA, USA) and imaged by high numerical aperture fluorescence microscopy on a TE2000 E2 inverted microscope system (Nikon instrument Inc., Melville, NY, USA) heated with an enclosed chamber (In Vivo Scientific, St. Louis, MO, USA). Timelapse images were captured by IPLab software to a cooled CCD camera (COOLSNAP HQ, Roper Scientific). Images were collected at 500–750 ms intervals using a PlanApo 60X NA 1.4 oil objective with exposure 200–500 ms at 2x2 binning. To determine the IFT particles velocities, time-lapse image sequences were assembled into kymographs using the ImageJ software package (http://rsbweb.nih.gov/ij). IFT velocities were analyzed in control and cell pre-treated for three hours with the appropriate compound.

Cyclic AMP Measurements

Confluent murine IMCD (inner medullary collecting duct), embryonically derived kidney epithelial cells (MEK) (untreated or treated with drugs) were lysed in 0.1 M HCl. Lysed samples were incubated at room temperature for 20 min. Samples were then transferred to the centrifuge tubes and spun at maximum speed in a tabletop microcentrifuge for 10 min. The supernatants were analyzed for cAMP via a direct immunoassay kit (BioVision Mountain View, CA, USA). The results were expressed as pmol of cAMP per μg of protein. The protein concentration was determined by using Bradford protein assay kit (Pierce, Rockford, IL, USA).

Statistical Analysis

Cilia length, IFT velocities, cAMP and calcium measurements were analyzed using by one-way analysis of variance test (ANOVA) using OriginPro 7.5 (OriginLab Corp., Northampton, MA, USA). All results were expressed as mean ± standard deviation (data from ≥ 3 independent experiments). Results were considered significant at $P<0.05$.

Supplementary Material

Refer to Web version on PubMed Central for supplementary material.

Acknowledgments

We thank Brad Yoder (University of Alabama, Birmingham, AB, USA) for IFT88/Polaris antibodies and Sangeeta Bhatia (Massachusetts Institute of Technology, Cambridge, MA, USA) for providing the laminar flow chamber. T.Y.B. and J.V.S. thank David Beier and Brad Yoder for critical reading of the manuscript; Ayumi Takakura, and members of the Shah laboratory and the Harvard PKD Center for helpful discussions. This work was partially supported by NIH Grant DK51050 to J.Z., NIH Grant AR36819 to B.R.O and the NIH-sponsored Harvard PKD Centre (P50DK074030) to J.V.S.

Abbreviations

IFT	Intraflagellar Transport
cAMP	3′-5′-cyclic adenosine monophosphate
ADPKD	Autosomal dominant polycystic kidney disease
PC1	Polycycstin-1
PC2	Polycystin-2

Literature Cited

1. Gerdes JM, Davis EE, Katsanis N. The vertebrate primary cilium in development, homeostasis, and disease. Cell 2009;137:32–45. [PubMed: 19345185]
2. Satir P, Christensen ST. Overview of structure and function of mammalian cilia. Annu Rev Physiol 2007;69:377–400. [PubMed: 17009929]
3. Marshall WF, Qin H, Rodrigo Brenni M, Rosenbaum JL. Flagellar length control system: testing a simple model based on intraflagellar transport and turnover. Mol Biol Cell 2005;16:270–278. [PubMed: 15496456]
4. Rosenbaum JL, Moulder JE, Ringo DL. Flagellar elongation and shortening in Chlamydomonas. The use of cycloheximide and colchicine to study the synthesis and assembly of flagellar proteins. J Cell Biol 1969;41:600–619. [PubMed: 5783876]
5. Rauchman MI, Nigam SK, Delpire E, Gullans SR. An osmotically tolerant inner medullary collecting duct cell line from an SV40 transgenic mouse. Am J Physiol 1993;265:F416–424. [PubMed: 8214101]
6. Nauli SM, Alenghat FJ, Luo Y, Williams E, Vassilev P, Li X, Elia AE, Lu W, Brown EM, Quinn SJ, Ingber DE, Zhou J. Polycystins 1 and 2 mediate mechanosensation in the primary cilium of kidney cells. Nat Genet 2003;33:129–137. [PubMed: 12514735]
7. Kolpakova-Hart E, McBratney-Owen B, Hou B, Fukai N, Nicolae C, Zhou J, Olsen BR. Growth of cranial synchondroses and sutures requires polycystin-1. Dev Biol 2008;321:407–419. [PubMed: 18652813]
8. Low SH, Roche PA, Anderson HA, van Ijzendoorn SC, Zhang M, Mostov KE, Weimbs T. Targeting of SNAP-23 and SNAP-25 in polarized epithelial cells. J Biol Chem 1998;273:3422–3430. [PubMed: 9452464]
9. Leuenroth SJ, Okuhara D, Shotwell JD, Markowitz GS, Yu Z, Somlo S, Crews CM. Triptolide is a traditional Chinese medicine-derived inhibitor of polycystic kidney disease. Proc Natl Acad Sci USA 2007;104:4389–4394. [PubMed: 17360534]
10. Mukhopadhyay S, Lu Y, Shaham S, Sengupta P. Sensory signaling-dependent remodeling of olfactory cilia architecture in C. elegans. Dev Cell 2008;14:762–774. [PubMed: 18477458]
11. Defer N, Best-Belpomme M, Hanoune J. Tissue specificity and physiological relevance of various isoforms of adenylyl cyclase. Am J Physiol Renal Physiol 2000;279:F400–416. [PubMed: 10966920]
12. Kozminski KG, Johnson KA, Forscher P, Rosenbaum JL. A motility in the eukaryotic flagellum unrelated to flagellar beating. Proc Natl Acad Sci USA 1993;90:5519–5523. [PubMed: 8516294]
13. Tran PV, Haycraft CJ, Besschetnova TY, Turbe-Doan A, Stottmann RW, Herron BJ, Chesebro AL, Qiu H, Scherz PJ, Shah JV, Yoder BK, Beier DR. THM1 negatively modulates mouse sonic

hedgehog signal transduction and affects retrograde intraflagellar transport in cilia. Nat Genet 2008;40:403–410. [PubMed: 18327258]

14. Engel B, Ludington W, Marshall W. Intraflagellar transport particle size scales inversely with flagellar length: revisiting the balance-point length control model. The Journal of Cell Biology 2009;187:81. [PubMed: 19805630]
15. Pan X, Ou G, Civelekoglu-Scholey G, Blacque OE, Endres NF, Tao L, Mogilner A, Leroux MR, Vale RD, Scholey JM. Mechanism of transport of IFT particles in C. elegans cilia by the concerted action of kinesin-II and OSM-3 motors. J Cell Biol 2006;174:1035–1045. [PubMed: 17000880]
16. Reed NA, Cai D, Blasius TL, Jih GT, Meyhofer E, Gaertig J, Verhey KJ. Microtubule acetylation promotes kinesin-1 binding and transport. Curr Biol 2006;16:2166–2172. [PubMed: 17084703]
17. Xu C, Shmukler BE, Nishimura K, Kaczmarek E, Rossetti S, Harris PC, Wandinger-Ness A, Bacallao RL, Alper SL. Attenuated, flow-induced ATP release contributes to absence of flow-sensitive, purinergic Ca2+ signaling in human ADPKD cyst epithelial cells. Am J Physiol Renal Physiol. 2009
18. Masyuk AI, Masyuk TV, Splinter PL, Huang BQ, Stroope AJ, Larusso NF. Cholangiocyte cilia detect changes in luminal fluid flow and transmit them into intracellular Ca2+ and cAMP signaling. Gastroenterology 2006;131:911–920. [PubMed: 16952559]
19. Praetorius HA, Spring KR. Bending the MDCK cell primary cilium increases intracellular calcium. J Membr Biol 2001;184:71–79. [PubMed: 11687880]
20. González-Perrett S, Kim K, Ibarra C, Damiano AE, Zotta E, Batelli M, Harris PC, Reisin IL, Arnaout MA, Cantiello HF. Polycystin-2, the protein mutated in autosomal dominant polycystic kidney disease (ADPKD), is a Ca2+-permeable nonselective cation channel. Proc Natl Acad Sci USA 2001;98:1182–1187. [PubMed: 11252306]
21. Harris PC, Torres VE. Polycystic Kidney Disease. Annu Rev Med. 2008
22. Wilson NF, Iyer JK, Buchheim JA, Meek W. Regulation of flagellar length in Chlamydomonas. Seminars in Cell & Developmental Biology 2008;19:494–501. [PubMed: 18692148]
23. Nauli SM, Zhou J. Polycystins and mechanosensation in renal and nodal cilia. Bioessays 2004;26:844–856. [PubMed: 15273987]
24. Verghese E, Weidenfeld R, Bertram J, Ricardo S, Deane J. Renal Cilia Display Length Alterations Following Tubular Injury and are Present Early in Epithelial Repair. Nephrol Dial Transplant. 2007
25. Verghese E, Ricardo SD, Weidenfeld R, Zhuang J, Hill PA, Langham RG, Deane JA. Renal Primary Cilia Lengthen after Acute Tubular Necrosis. Journal of the American Society of Nephrology 2009:1–7.
26. Patel V, Li L, Cobo-Stark P, Shao X, Somlo S, Lin F, Igarashi P. Acute kidney injury and aberrant planar cell polarity induce cyst formation in mice lacking renal cilia. Hum Mol Genet 2008;17:1578–1590. [PubMed: 18263895]
27. Happé H, Leonhard WN, van der Wal A, van de Water B, Lantinga-van Leeuwen IS, Breuning MH, de Heer E, Peters DJM. Toxic tubular injury in kidneys from Pkd1-deletion mice accelerates cystogenesis accompanied by dysregulated planar cell polarity and canonical Wnt signaling pathways. Human Molecular Genetics 2009;18:2532–2542. [PubMed: 19401297]
28. Takakura A, Contrino L, Zhou X, Bonventre JV, Sun Y, Humphreys BD, Zhou J. Renal injury is a third hit promoting rapid development of adult polycystic kidney disease. Human Molecular Genetics 2009;18:2523–2531. [PubMed: 19342421]

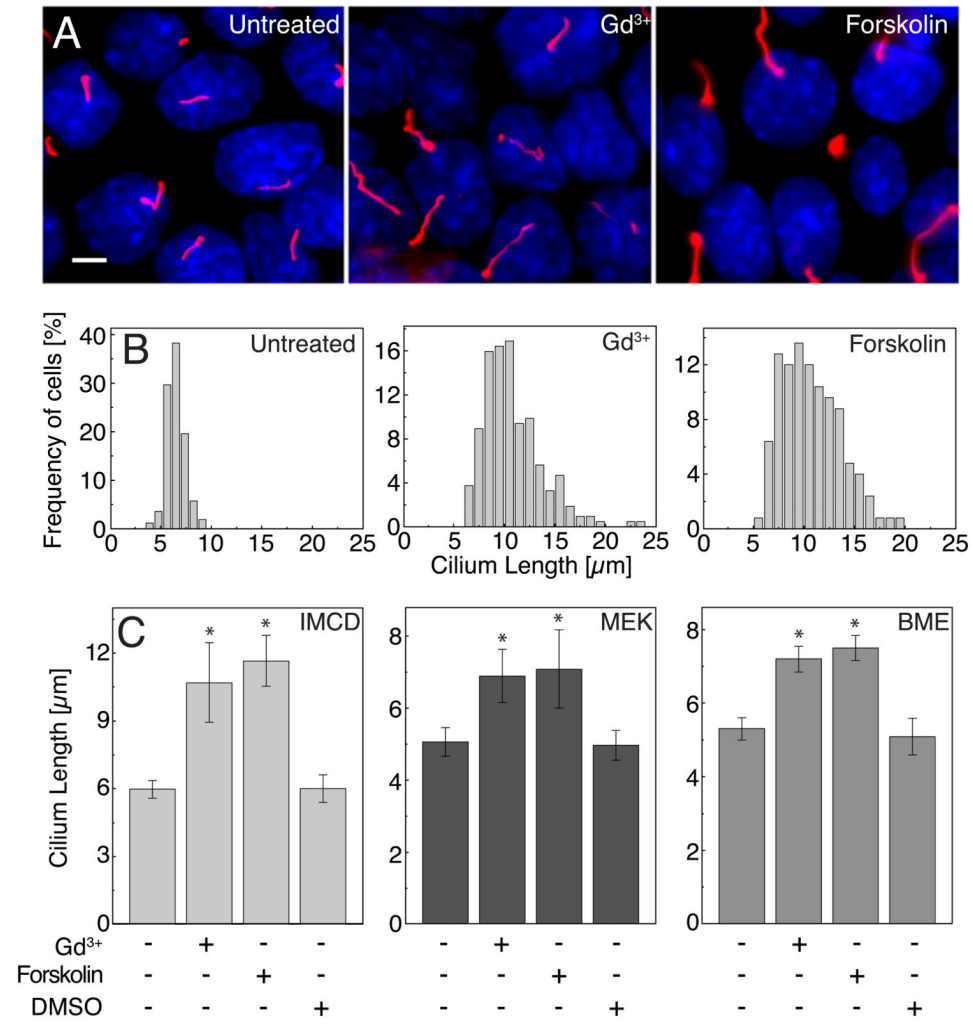

Figure 1. Increase of cilium length induced by modulation of intracellular cAMP and Ca^{2+} levels

(A) IMCD cells showed cilium elongation after increasing cAMP (100 μM forskolin) or inhibiting intracellular Ca^{2+} entry (30 μM Gd^{3+}) for three hours. Acetylated α-tubulin was used as a ciliary marker (red). Scale bar, 5μm. **(B)** Histograms of cilia length distribution in untreated and treated for 3 hours IMCD cells (n > 150). **(C)** Average length of cilia of IMCD, MEK and BME cells after 3 hours of drug treatment (*P< 0.001). Error bars indicate mean ± s.d.

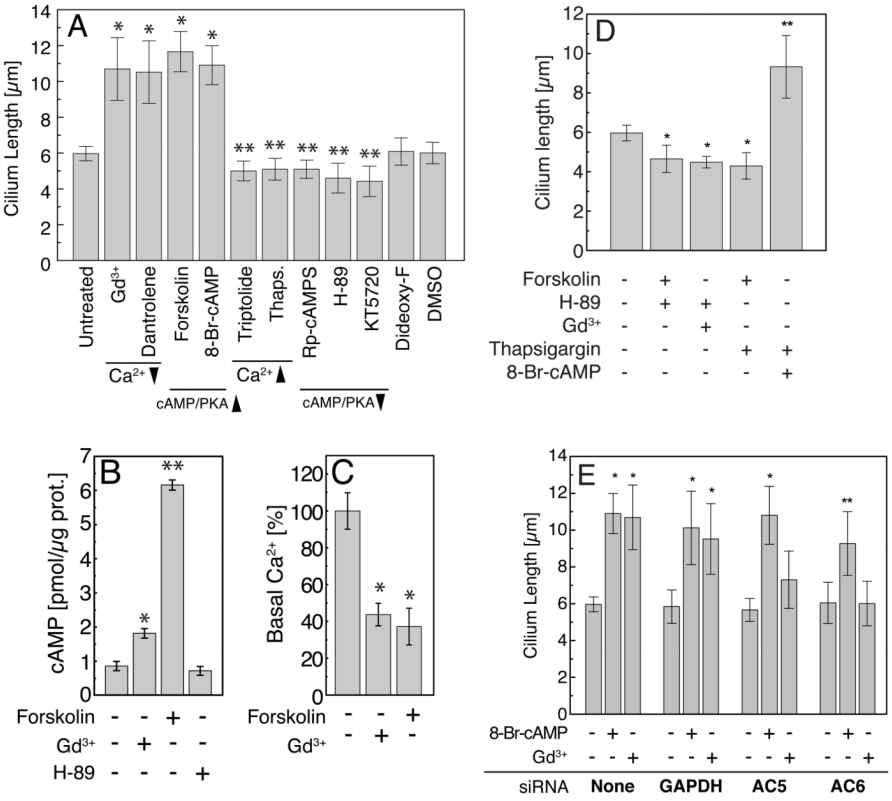

Figure 2. Pathway analysis of second messenger induced cilium length increase

(A) Cilium length increased after blockade of Ca^{2+} entry (Gd^{3+}), inhibition of Ca^{2+} release from intracellular stores (Dantrolene) and activation of adenylyl cyclases (Forskolin) or PKA (8-Br-cAMP). Activation of Ca^{2+} signaling by Triptolide or Thapsigargin or inhibition of PKA signaling (Rp-cAMPS, KT-5270, H-89) resulted in cilium length reduction. 1,9-dideoxy-Forskolin (Dideoxy-F) and DMSO are control treatments that did not affect cilium length; * P< 0.001; ** P< 0.05. All treatments were for three hours. **(B)** Gd^{3+} or forskolin treatment resulted in increased intracellular cAMP; *P< 0.01, **P< 0.001. **(C)** Steady-state levels of intracellular Ca^{2+} were reduced under treatment of Gd^{3+} or forskolin. **(D)** Inhibition of PKA along with Gd^{3+} or forskolin treatment resulted in cilium length reduction (*P< 0.05). The increase of intracellular calcium (Thapsigargin) suppressed the effect of direct adenylate cyclase activation (forskolin) on cilium length but had no effect on the cilia lengthening caused by the direct stimulation of PKA (8-Br-cAMP). **(E)** Silencing of AC5 or AC6 prevents cilium lengthening in response to Gd^{3+} but not PKA activation by 8-Br-cAMP. The bar graph represents the average length of cilia after 48 hours of siRNA-mediated knockdown, followed by 3 hours of drug treatment. siRNA GAPDH was used as a control for siRNA targeting. n=100, (*P< 0.001, **P< 0.05). Error bars indicate mean ± s.d.

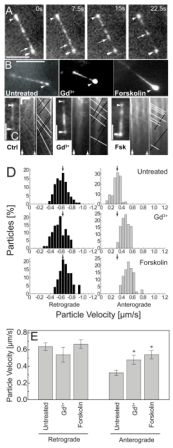

Figure 3. Anterograde IFT velocities increase under cilium lengthening

(A) Visualization of the IFT88-EYFP particles in live IMCD cells revealed a punctuate distribution throughout the ciliary axoneme. White arrows highlight particle movement (Cilium tip – Single arrowhead, Basal body – double arrowhead). Time given in seconds. Scale bar is 5 μm. **(B)** Drug treated cells show accumulation of IFT88 at the tips of primary cilia. Scale bar is 5 μm. **(C)** To determine the IFT particles velocities, time-lapse image sequences were assembled into kymographs. Black and white lines on the kymograph indicate anterograde and retrograde velocities, respectively. Length Scale bar (horizontal), 5μm. Time scale bar (vertical), 5 sec**. (D)** Histograms of the particle velocity in untreated and drug-treated cells. Negative velocities (left) represent retrograde particles, and positive velocities (right) indicate anterograde particles. Arrows represent mean velocity in untreated cells. **(E)** Ca^{2+} inhibition or cAMP activation increased anterograde velocity with no significant effect on retrograde velocity. Error bars indicate mean ± s.d.; *P< 0.001.

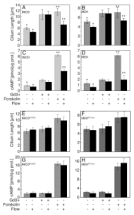

Figure 4. Cilium length and cAMP adaptation under flow depends on polycystins

(A, B) Untreated cells subjected to fluid flow (shear stress 0.75 dyne/cm^2) (light grey bars – IMCD no flow, dark grey bars – MEK no flow, black bars – flow) underwent a significant decrease in cilium length. Treatment with forskolin in combination with flow also reduced cilium length. Fluid flow did not suppress length increase caused by Gd^{3+}. **(C, D)** In untreated or forskolin stimulated cells cAMP levels were reduced under flow condition in wild-type cells. There was no change in cAMP in Gd^{3+} treated cells under flow. **(E, F)** Cilium length did not decrease under the application of flow to cells knocked down for PC-2 ($IMCD^{PC2KD}$) or harbouring genetic mutations in PC-1 (MEK^{PC1mut}) (hatched bars – no flow; black bars – flow) in either untreated or forskolin stimulated cells. In addition, $IMCD^{PC2KD}$ and MEK^{PC1mut} cells did not increase cilium length in response to Gd^{3+}. **(G, H)** cAMP levels were unchanged after flow in $IMCD^{PC2KD}$ and MEK^{PC1mut} cells or in response to Gd^{3+}. Error bars indicate mean ± s.d.*P<0.05; **P<0.001.